Dual optical cycling centers mounted on an organic scaffold: New insights from quantum chemistry calculations and symmetry analysis

Taras Khvorost,[1] Paweł Wójcik,[2] Cecilia Chang,[1] Mia Calvillo,[1] Claire Dickerson,[1] Anna I. Krylov,[2] and Anastassia N. Alexandrova[1, a)]

[1)] *Department of Chemistry and Biochemistry, University of California, Los Angeles, California 90095, USA*

[2)] *Department of Chemistry, University of Southern California, Los Angeles, CA 90089, USA*

(Dated: 24 January 2024)

Molecules cooled to the ultracold temperatures are desirable for applications in fundamental physics and quantum information science. However, cooling polyatomic molecules with more than six atoms has not yet been achieved. Building on the idea of an optical cycling center (OCC), a moiety supporting a set of localized and isolated electronic states within a polyatomic molecule, molecules with two OCCs (bi-OCCs) may afford a better cooling efficiency by doubling the photon scattering rate. By using quantum chemistry calculations, we assess the extent of the coupling of the two OCCs with each other and with the molecular scaffold. We show that promising coolable bi-OCC molecules can be proposed following chemical design principles.

[a)] Electronic mail: ana@chem.ucla.edu

Ultracold molecules are attractive for novel applications[1–3]. Molecules can be cooled to the ultracold temperatures by laser cooling, a repeated absorption and emission of photons exploiting the Doppler effect[4]. When excitation laser is tuned to energy slightly below the electronic transition, only molecules moving towards the photon source can be excited. The excited molecule then undergoes spontaneous decay by which it emits recoil momentum in all directions, slowing the average momentum over time. The key to laser-cooling molecules is the ability to prevent decay to unwanted decay channels, such as excited vibrational states. The process of scattering many photons using the same closed loop is called optical cycling. The undesirable population leakage into vibrationally excited states is minimized when ground and electronically excited states have the same structures, thereby resulting in the diagonal Franck-Condon factors (FCFs; vibrational overlaps). This goal can be achieved by designing molecules with localized atomic-like transitions, as was first described by Isaev and Berger[5], who also proposed several promising candidates—all based on a metal-oxygen-ligand (M-O-L) framework with a second-group metals. The essential features of these systems are a strongly ionic M-O bond and a localized unpaired electron on the metal, giving rise to localized atomic-like transitions. These transitions can be used as the main photon cycling loop; hence, the name optical cycling center (OCC).

Several molecules featuring such electronic structure have been successfully laser-cooled[6–8]. Cooling larger molecules could be advantageous for quantum information and sensing applications[9–11]. Although initially the enthusiasm was dampened by the concerns that the increased complexity is likely to result in more vibrational branching channels, several theoretical studies have shown that such metal-based OCCs can in fact operate in larger molecules. Following this strategy, more polyatomic molecules were proposed computationally as prospective candidates for laser cooling[12–21]. The screening of the candidate molecules entails finding a low-lying bright electronic transition, assessing that it is electronically uncoupled from the rest of the molecule, and computing FCFs (vibrational overlaps). The electronic transitions and FCFs can be tuned using chemical intuition. As recent studies show, strongly diagonal FCFs are possible in large molecules, leading to vibrational branching ratios rivaled that of CaOH[17–19].

It is desirable to further optimize photon cycling in the candidate molecules, such that one can use fewer repump lasers, introduce additional optical controls, and explore more varied types of molecules. One way to increase cycling efficiency is to install multiple OCCs

on one scaffold, which can increase the oscillator strength, potentially doubling the photon scatters[13,15,22,23]. Here, we explore this idea further, by considering a larger set of molecular scaffolds augmented by two OCCs (we refer to them as bi-OCCs). We analyze the effect of symmetry and use chemical design to control the optical properties of the prospective bi-OCCs and the respective FCFs (FCFs control vibrational branching ratios in electronic transitions).

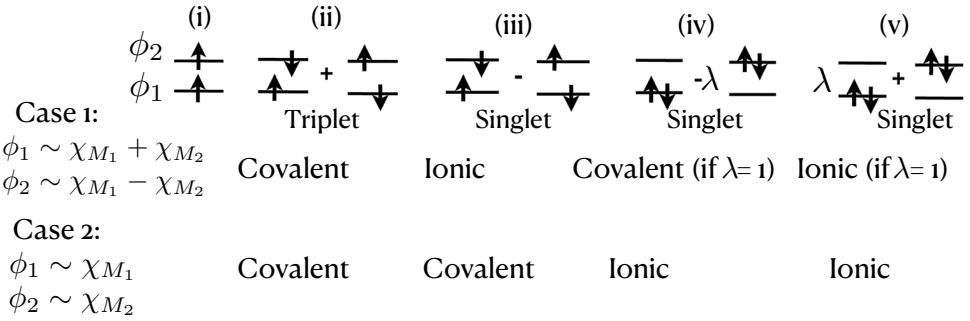

FIG. 1. Diradicals: Different electronic configurations derived from distributing two electrons in two orbitals and their characters. M_1 and M_2 denote two radical centers, e.g., the two metal atoms in bi-OCCs. Configuration (i) is the high-spin (M_s=1) triplet state and configurations (ii)-(v) are low-spin (M_s=1) states. Case 1 corresponds to perfectly delocalized frontier orbitals (such as bonding and antibonding combinations of atomic orbitals) and Case 2 corresponds to the molecular orbitals perfectly localized on the radical centers.

Although bi-OCC molecules may seem exotic, many features of their electronic structure can be understood by revisiting diradicals.[24–28] Diradicals are species in which the two frontier molecular orbitals are (nearly)-degenerate and the low-lying electronic states derived by distributing two electrons in two orbitals. Fig. 1 shows resulting electronic configurations. The character of the wave-functions depends whether the orbitals are delocalized or localized. The triplet states are always covalent—they correspond to the unpaired electrons localized on the two metal centers whereas the singlets can be either covalent, ionic ($M_1^+M_2^- \pm M_2^-M_1^+$), or a mixture of covalent and ionic (charge-resonance) contributions. Considering delocalized orbitals (case 1 in Fig. 1), configuration (iv) corresponds to purely covalent diradical configuration with two unpaired electrons when λ=1 and to an equal mixture of ionic and covalent configurations when λ=0. The extent of diradical character of the wave-function can be quantified by computing the number of effectively unpaired electrons,

$n_{u,nl}$, using Head-Gordon's formula[29]. In the triplet state (configurations (i) and (ii)), the number of unpaired electrons is 2. For configuration (iv) and delocalized orbitals (case 1 in Fig. 1), the number of unpaired electrons can be computed from the parameter λ as follows[28]:

$$n_{u,nl} = \frac{32\lambda^4}{(1+\lambda^2)^4}. \quad (1)$$

Energy gap between the frontier orbitals controls parameter λ and the relative energies of the lowest singlet and triplet states—lager gaps favor ground singlet states. If the energy separation between ϕ_1 and ϕ_2 states is very small, the triplet can become the ground state. The gap depends on the through-space and through bond interactions. Through-space interaction depends on the overlap of the contributing atomic orbitals whereas through-bong interaction depends on the molecular scaffold and the relative placements of the radical centers. This may lead to flipping the ground-state multiplicity in structural isomers—for example, meta-xylylenes have triplet ground state whereas para-xylylene have singlet ground state.

Previous studies of bi-OCCs considered the following motifs—M1-CC-M2, with M1/M2=Mg,Ca,Sr (Ref. 13) and M1=Yb and M2-Ca/Al (Ref. 22), benzenes functionalized by Ca in ortho-, meta-, and para- positions[15], as well as Sr and OSr installed on $(CH_2)_n$ chains and fullerenes (Ref. 23). These studies revealed the following essential features of bi-OCCs:

- Even in the systems with a short acetylene linker, the frontier orbitals are localized on metal centers and the low-lying electronic states are largerly uncoupled from the scaffold; this can be explained by the large energy gap between the metal and linker orbitals and the diffuse nature of the former.

- Both through-space and through-bond interactions between the two centers are weak, leading to nearly or almost degenerate singlet and triplet states.

- Because of the weak interaction between the OCCs, the characters of the singlet and triplet states are similar—both are covalent (i.e., $n_{u,nl}$ $\geq$1.8 for the lowest singlet states). Furthermore, the low-lying excited states in each multiplicity follow nearly identical patterns. The energy spacing follows that of a single OCC very closely, with very small excitonic splitting.

- In bi-OCCs with the short acetylenic linker, the coupling between the centers and the

linker and between the centers themselves is smaller for heavier metals for which the two manifolds become even more similar. However, in phenoxide with a single OCC, Sr resulted in worse FCFs than Ca.[30]

In high-symmetry cases, excited states show excitonic patterns, with one state dark and one carrying double oscillator strength of a single OCC. Depending on the structure, the lowest excited state can be either bright (desirable for cycling) or dark (undesirable). This can be understood in the framework of the exciton model[31,32]—if the transition moments of the two chromophores are parallel but not aligned, one obtains an H-dimer in which the lowest state is dark. If the two moments are aligned along the same axis, one obtains a J-dimer in which the lowest state is bright (super-radiant).

The lowest transitions in the metal-based OCCs are of $s \rightarrow p$ types, with the p-orbital aligned along the MO bond being hybridized with the respective d-orbital. The transition moments are aligned along the direction of the corresponding p-orbitals. Hence, the excitonic pattern can be controlled by splitting the degeneracy of the p-orbitals and their relative orientation in a molecule. Specifically, in p-benzyne bi-OCC, the lowest transition is dark and in m- and o-benzynes it is bright (but not super-radiant).

Here we use M-O-X framework, in which the metal centers are even further apart, thus improving the decoupling relative to the M-X motifs. Fig. 2 shows the bi-OCC molecules studied in this work.

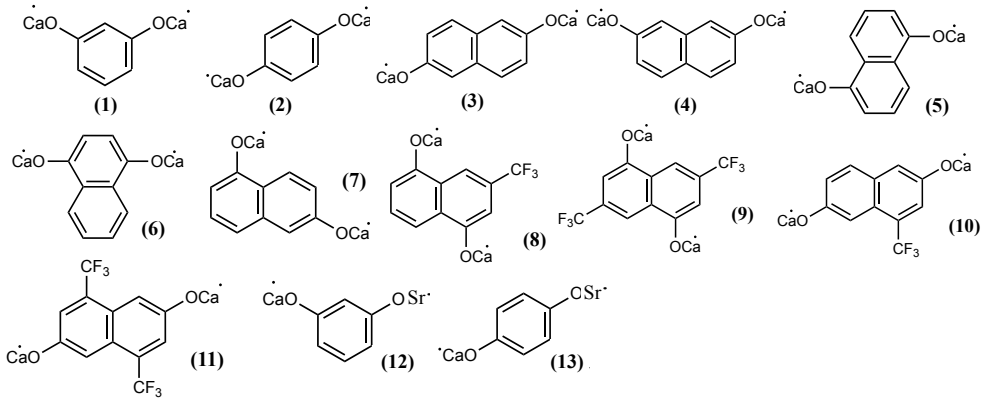

FIG. 2. Structures of bi-OCC molecules considered in this work.

The type of electronic structure featured by OCCs can be accurately described by the double electron attachment variant[33] of equation-of-motion coupled-cluster methods[34] in which the ground and excited target states are described by attaching two electrons to

a dicationic reference, as was done in Refs. 12,13. Here we use EOM-DEA-CCSD with the cc-pVDZ basis on H,C,O and aug-cc-pwCVDZ-PP on Ca and Sr with the ECP10MDF and ECP28MDF pseudopotentials used for the respective metal atoms. EOM-DEA-CCSD calculations were carried out using Q-Chem[35].

For extensive screening involving calculations of FCFs for relatively large molecules it is desirable to develop a less expensive protocol. Here we take advantage of the fact that lowest singlet and triplet manifolds of bi-OCCs have very similar character. Hence, one can use triplet manifold as a proxy for singlet states. Whereas low-spin singlet and triplet states are multi-configurational, the high-spin triplet states can be well described by a single-reference method (HF, CCSD, DFT), which is exploited, for example, in spin-flip approach[36,37]. Following the same logic, here we compute the triplet-state manifold from the lowest high-spin triplet state using density functional theory (DFT) and its extension to the excited states, TD-DFT. We use the PBE0-D3/def2-TZVPPD level of theory for geometry optimizations, excitations, frequencies, and FCFs, as implemented in Gaussian16[38–41]. The validate this approach, we benchmarked it against EOM-DEA-CCSD; the results are given in the SI.

We begin by discussing benzenes functionalized by two Ca-O OCCs installed in meta- (**(1)**) and para- (**(2)**) positions (see Fig. 2). This builds upon previous work where we experimentally realized the single OCC case, CaOPh[17].

The natural orbitals hosting the unpaired electrons are in-phase and out-of-phase combinations of the *s*- and *p*-orbitals of the to Ca atoms (Fig. 3). The ground state is derived by distributing two electrons in the molecular orbitals derived by linear combinations of the two *s*-orbitals. The lowest triplet states are $^3B_1$ in **(1)** and $^3B_{3u}$ in **(2)**; they appear to be degenerate with the lowest singlet states ($^1A_1$ and ^1A_g) at the EOM-DEA-CCSD level of theory. The wave-function analysis yields $n_{u,nl}$=2 for the singlet states, confirming that the singlet state has pure diradical character. We note that for the analogous Ca-substituted benzenes[15], $n_{u,nl}$ values were smaller—1.83, 1.92, and 2.00 for ortho-, meta-, and para-isomers, respectively. Hence, linking metals through the oxygen improves the decoupling of the unpaired electrons and reduces ionic contributions, which should improve the FCFs. This effective decoupling also makes singlets electronically very similar to the triplets. Hence, we expect that the cycling efficiency should not be affected by the transitions between the two spin manifolds, which can be induced by spin–orbit coupling.

Excited-state properties of **(1)** and **(2)** can be rationalized using symmetry analysis.

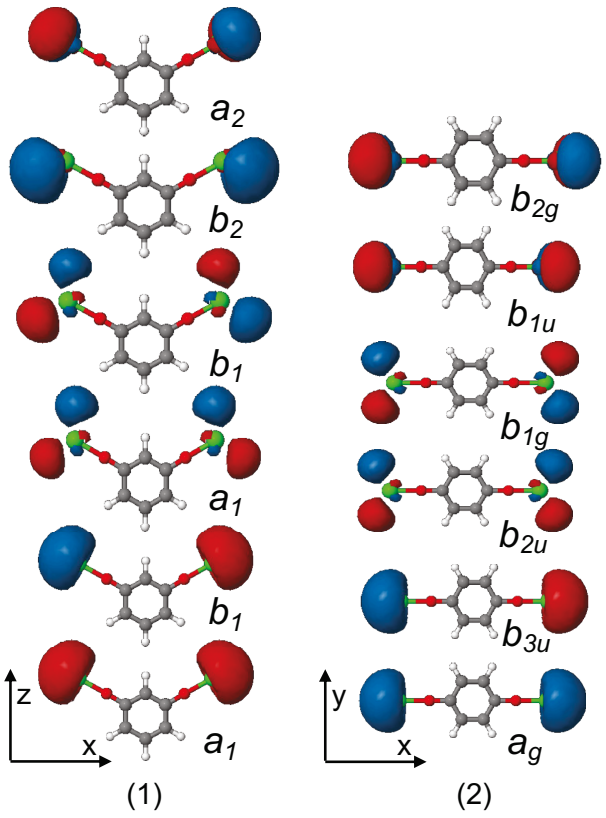

FIG. 3. Frontier orbitals and their symmetries for the two simplest bi-OCC molecules — Ca-O-Ph-3-O-Ca with C_{2v} point group **(1)** and Ca-O-Ph-4-O-Ca with D_{2h} point group **(2)**. Note: Symmetry labels correspond to Q-Chem's standard molecular orientation[42]. EOM-DEA-CCSD/cc-pVDZ[H,C,O]/aug-cc-pwCVDZ-PP[Ca]/ECP10MDF[Ca]; isovalue 0.03.

The OCC transitions are derived by promoting electrons to the molecular orbitals derived from a pair of p-orbitals. The degeneracy between the atomic p-orbitals is lifted such that the lowest p-orbitals are in-plane, perpendicular to the Ca-O bond, followed by the out-of-plane orbitals, and p-orbitals parallel to the Ca-O bond (these highest pair of orbitals is not shown in Fig. 3). Using point-group symmetry, we can then determine the number of bright transitions for a given OCC molecule. For example, in **(1)** (C_{2v}) combinations of s-orbitals have a_1 and b_1 symmetries, and combinations of p-orbitals have a_1, b_1, b_2, and a_2 symmetries. One of the in-plane excited states is derived by $a_1 \rightarrow a_1$ and $b_1 \rightarrow b_1$ transitions, yielding bright transition of A_1 symmetry. Transition $a_1 \rightarrow b_1$ (of B_1 symmetry) is also optically allowed. Similarly, two out-of-plane transitions have B_1 and A_2 symmetries, rendering the latter one dark. We remind that for the transitions from $^1A_1$, the symmetry of the target

state is the same as the symmetry of the transition whereas for the transitions from the open-shell triplet state, the symmetry of the target state is the product of the symmetry of the transition and the initial triplet state ($^3B_1$ in **(2)**). Following the same analysis, in **(2)**, (D_{2h}), we anticipate two bright transitions—B_{1u} and B_{2u}. Unfortunately, as anticipated from the orbital pictures, the lowest states correspond to H-aggregate type, rendering the lowest excited states dim in **(1)** and optically forbidden in **(2)**.

Table I shows the results for **(1)** and **(2)** for the lowest transitions in the triplet manifold and the respective oscillator strength. As anticipated from our analysis, **(1)** has three bright transitions with symmetries B_1, A_1, and B_2 (corresponding to $^3A_1$, $^3B_1$, and $^3A_2$ states). The lowest state is optically allowed, but not very bright (f_l=0.126). The respective FCF, $^3A_1(\nu = 0) \rightarrow ^3B_1(\nu = 0)$, is almost twice smaller than that of the fundamental transitions from the $^3B_1$ and $^3A_2$ states (0.5051 versus 0.9176 and 0.9604). Previously, some of us investigated this effect and found that the diagonality of FCFs is improving proportionally to the distance between the optical centers.[43]

TABLE I. Properties of four lowest excited states[a] of **(1)** and **(2)** in the triplet manifold; the lowest triplet state is $^3B_1$ and $^3B_{3u}$, respectively.

(1) Ca-O-Ph-3-O-Ca			**(2)** Ca-O-Ph-4-O-Ca		
State	E_{ex}, eV (f_l)	FCF	State	E_{ex}, eV (f_l)	FCF
1^3A_1	2.036 (0.126)	0.5051	1^3B_{2u}	2.044 (—)	—
1^3B_2	2.058 (—)	—	1^3B_{1u}	2.060 (—)	—
2^3B_1	2.085 (0.401)	0.9176	1^3B_{1g}	2.066 (0.518)	0.9663
1^3A_2	2.097 (0.543)	0.9604	1^3B_{2g}	2.085 (0.544)	0.9792

[a] Excitation energies and oscillator strengths: EOM-DEA-CCSD/cc-pVDZ[H,C,O]/aug-cc-pwCVDZ-PP[Ca]/ECP10MDF[Ca]; FCFs: PBE0-D3/def2-TZVPPD.

(2) has two highly diagonal bright states of symmetries B_{1g} and B_{2g} with FCFs 0.9663 and 0.9792, respectively. The oscillator strengths of **(2)**'s bright transitions are roughly twice as large as the oscillator strength of the single-OCC CaOPh molecule (0.518 and 0.544 in bi-OCC versus 0.2075 and 0.2155 in single-OCC) and two subradiant states[44], following the same pattern as in Ca-X species[13]. Unfortunately, the lowest transition is dark because

of the H-dimer arrangement. In order to obtain superradiant lowest states in these two model systems, the energies of the two highest molecular orbitals, which are derived from the hybridized p and d orbitals parallel to the Ca-O bond, have to be brought below the other orbitals in the p-manifold, which might be possible to achieve by using bulky substituents that destabilize the other four orbitals. However, given the small size of the benzene scaffold, this route is impractical as such substituents would deteriorate FCFs.

Overall, bi-OCC molecules are good candidates for laser cooling purposes because of good FCFs and the flexibility they afford to tune excited states. Because the phenyl ring does not allow for complex functionalization—even a small substituents (such as a CH_3 group) interferes with the Ca-centered orbitals, reducing FCFs and increasing orbital mixing (see Supplementary Information)—we turn to the larger scaffolds, such as naphthalene (systems **(3)-(11)** in Fig. 2). Naphthalene and its structural isomer azulene, were previously considered in its unfunctionalized version for buffer-gas cooling.[45] Below we demonstrate how various structural modifications affect optical properties of bi-OCCs, allowing one to enhance or disentangle relevant electronic transitions.

TABLE II. Excitation energies (eV), oscillator strengths (in parentheses), and FCFs for the 0→0 transition for different excited states in the triplet manifold for **(3) - (11)**[a]. The symmetry of the lowest triplet state for each system is given next to the system number.

(3) 1^3B_u			**(8)** $1^3A'$		
2^3B_u	1.991 (—)	—	$2^3A'$	2.092 (0.077)	0.9145
1^3A_g	2.005 (0.518)	0.9668	$1^3A''$	2.099 (0.013)	0.9603
1^3A_u	2.015 (—)	—	$3^3A'$	2.120 (0.417)	0.9657
1^3B_g	2.030 (0.550)	0.9815	$2^3A''$	2.123 (0.513)	0.9831
(4) 1^3B_1			**(9)** 1^3B_u		
1^3A_1	1.987 (0.123)	0.9264	1^3A_u	2.123 (—)	—
1^3B_2	2.013 (—)	—	2^3B_u	2.130 (—)	—
2^3B_1	2.013 (0.400)	0.9646	1^3B_g	2.145 (0.523)	0.9855
1^3A_2	2.035 (0.550)	0.9796	1^3A_g	2.149 (0.493)	0.8048
(5) 1^3B_u			**(10)** $1^3A'$		
2^3B_u	1.994 (—)	—	$2^3A'$	2.074 (0.0002)	0.9619
1^3A_g	2.014 (0.504)	0.9631	$3^3A'$	2.087 (0.507)	0.9721
1^3A_u	2.020 (—)	—	$1^3A''$	2.089 (0.015)	0.9793
1^3B_g	2.044 (0.540)	0.9817	$2^3A''$	2.105 (0.525)	0.9846
(6) 1^3B_1			**(11)** 1^3B_u		
1^3A_1	1.979 (0.0001)	0.9409	2^3B_u	2.090 (—)	—
2^3B_1	2.006 (0.503)	0.9649	1^3A_u	2.100 (—)	—
1^3B_2	2.014 (—)	—	1^3A_g	2.103 (0.505)	0.951
1^3A_2	2.039 (0.540)	0.9354	1^3B_g	2.115 (0.536)	0.970
(7) $1^3A'$					
$2^3A'$	1.984 (0.143)	0.8583			
$1^3A''$	2.013 (0.007)	0.9631			
$3^3A'$	2.015 (0.381)	0.9547			
$2^3A''$	2.042 (0.538)	0.9845			

[a]Excitation energies and oscillator strengths: EOM-DEA-CCSD/cc-pVDZ[H,C,O,F]/aug-cc-pwCVDZ-PP[Ca]/ECP10MDF[Ca]; FCFs: PBE0-D3/def2-TZVPPD.

Table II presents the results for naphthalene-based bi-OCCs (see Fig. 2). The naphthalene molecule has three types of symmetry non-equivalent carbon atoms where we can install an OCC, giving rise to the following five bi-OCC structures: four molecules with OCCs on equivalent carbon sites (systems **(3)**, **(4)**, **(5)**, and **(6)**) and one molecule with OCCs on non-equivalent sites (system **(7)**). In these systems, the lowest singlet and triplet are also degenerate (at the EOM-DEA-CCSD level), and the number of effectively unpaired electrons in the lowest singlet state is two.

With these arrangements, we observe different patterns of how the combined oscillator strength derived from the $s \rightarrow p$ transitions is distributed among low-lying manifold of excited states. In systems with high symmetry, the oscillator strength is concentrated in a smaller number of states whereas in low-symmetry cases it is distributed among more states so that in non-symmetric cases the number of optically allowed states is the largest. As for **(1)** and **(2)**, symmetry considerations explain the results for these larger systems. Systems **(3)** and **(5)** have the C_{2h} symmetry and two bright states. **(4)** and **(6)** have the C_{2v} symmetry and three bright states whereas **(7)** has the C_s symmetry and four bright states.

For C_{2h} systems, both bright states are superradiant (the oscillator strength is on the order of 0.5, which is twice larger than that in single-OCC molecules), whereas for C_{2v} systems there are two super- and one sub-radiant states, with the latter having low oscillator strength (0.123 for **(4)**, and 0.0001 for **(6)**). For system **(7)**, both super- and sub- radiant states are bright. Here again the brighter states appear higher in energy, which is not suitable for optical cycling.

As was previously shown, electron-withdrawing groups with high Hammett parameters improve FCFs for single-OCC transitions for benzenes and naphthalenes[17,46]. We extend this idea to their bi-OCC counterparts by functionalizing two of the five systems with electron-withdrawing CF_3 groups (systems **(8)-(11)**). We functionalized systems **(3)** and **(5)** because the substituents are positioned at a distance away from the OCCs such that they do not disrupt the OCC transitions. We then functionalized **(3)** and **(5)** by one or two substituents to produce systems **(10)**, **(11)** and **(8)**, **(9)**, respectively, to investigate stronger electron-withdrawing effects.

For singly CF_3 functionalized systems, **(8)** and **(10)**, all four excited states are bright due to C_s symmetry point group, similar to system **(7)**. The first excited A′ and A″ states are

subradiant (with oscillator strengths less than 0.1). For **(8)**, the superradiant transitions (to the third and fourth excited states) have FCFs of 0.9657 and 0.9831, an improvement over the corresponding ground to excited state transitions of their unfunctionalized counterpart, **(5)** (0.9631 and 0.9817). Similarly, **(10)**'s superradiant transitions have FCFs of 0.9721 and 0.9846, an improvement over **(3)**'s (FCFs of 0.9668 and 0.9815).

Double functionalization with CF_3 (systems **(9)** and **(11)**) recovers the symmetry of the parent species and, consequently, their numbers of bright excited states. However, the FCFs for doubly functionalized species deteriorate slightly. This is because functionalization often introduces more vibrational degrees of freedom that electronic states can couple to, even while improving on the order of this coupling by utilizing electronic effects. For example, the first two decay channels for the B_u transition of **(5)** are decays to the stretching and bending modes with FCFs of 0.0132 and 0.0124, respectively. For the B_u transition of **(9)** the two main channels are also stretching and bending, but with FCFs of 0.0041 and 0.0035, respectively. The same characteristic applies to **(11)** and **(3)**. This means that we succeed in improving the diagonality of the transition electronically, however, in this particular case the introduced vibrational degrees of freedom quench that effect and ultimately result in worsening of FCF. This suggests to consider exploring heteroatomic motifs in future work—e.g., introducing nitrogen or boron in the scaffold can significantly affect electronic states (as was observed in organic di- and tri-radicals[47–49]), but without introducing more degrees of freedom.

TABLE III. Properties of four lowest excited states of **(12)** and **(13)** in the triplet manifold[a]; the lowest triplet state is $1^3\mathrm{A}'$ and 1^3A_1, respectively.

(12) Ca-O-Ph-3-O-Sr				**(13)** Ca-O-Ph-4-O-Sr			
State	E_{ex}, eV	(f_l)	FCF	State	E_{ex}, eV	(f_l)	FCF
$2^3\mathrm{A}'$	1.762	(0.261)	0.8122	1^3B_1	1.627	(0.274)	0.9057
$1^3\mathrm{A}''$	1.784	(0.251)	0.9293	1^3B_2	1.656	(0.283)	0.9279
$3^3\mathrm{A}'$	2.045	(0.378)	0.9256	2^3A_1	1.918	(0.278)	0.9325
$2^3\mathrm{A}''$	2.066	(0.165)	0.9594	2^3B_1	2.071	(0.275)	0.9538

[a] Excitation energies and oscillator strengths: EOM-DEA-CCSD/cc-pVDZ[H,C,O]/aug-cc-pwCVDZ-PP[Ca,Sr]/ECP10MDF[Ca]/ECP28MDF[Sr]; FCFs: PBE0-D3/def2-TZVPPD.

Additional flexibility in laser-coolable bi-OCCs is afforded by using different metals,[13,22] which makes the two centers distinguishable and independently addressable. Table III and Figs. 4 and 5 show the results for the systems with one Ca and one Sr OCCs (systems **(12)** and **(13)** in Fig. 2). As we can see from the natural orbitals, electronic transitions are localized, so that they can be addressed individually. This is different from the bimetallic bi-OCCs linked through the short acetylene bridge[13] where the transitions showed some degree of delocalization, consistent with stronger interactions between the two centers.

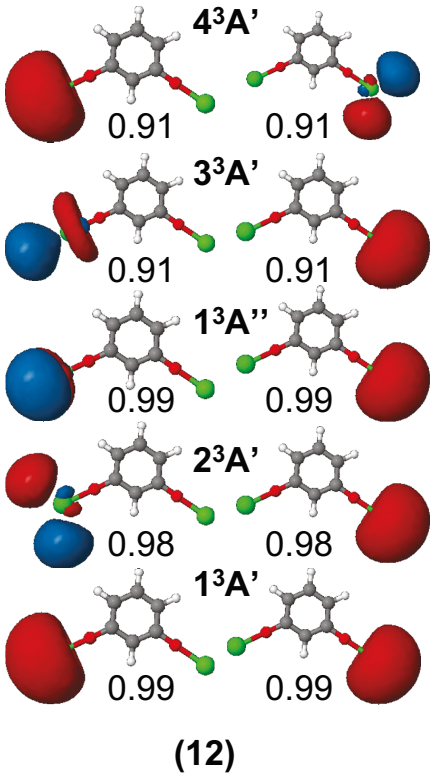

FIG. 4. Natural orbitals and their occupations for the lowest triplet states of a mixed bi-OCC CaO-Ph-3-OSr **(12)**. EOM-DEA-CCSD/cc-pVDZ[H,C,O]/aug-cc-pwCVDZ-PP[Ca,Sr]/ECP10MDF[Ca]/ECP28MDF[Sr]; isovalue 0.03.

In this contribution, we investigated details of the electronic structure of bi-OCCs. We have shown that in bi-OCCs built upon benzene and naphthalene scaffolds by augmenting them with two OM groups (M=Ca, Sr), the two optical centers are decoupled from each other and from the organic scaffold, giving rise to degenerate perfect diradical singlet and triplet ground states. In the future work, we will investigate whether this degeneracy is lifted when higher correlation treatment is employed and spin–orbit interaction is accounted for.

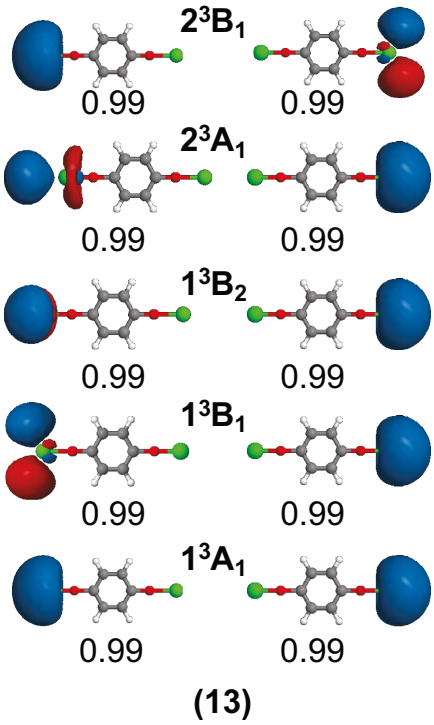

FIG. 5. Natural orbitals and their occupations for the lowest triplet states of a mixed bi-OCC CaO-Ph-3-OSr **(13)**. EOM-DEA-CCSD/cc-pVDZ[H,C,O]/aug-cc-pwCVDZ-PP[Ca,Sr]/ECP10MDF[Ca]/ECP28MDF[Sr]; isovalue 0.03.

We expect that the multiplicity of the ground states in these systems is not important, as the lowest singlet and triplet states are very similar electronically. Moreover, the singlet and triplet manifolds of excited states are also very similar. Thus, we expect that the transitions between the two manifolds should not pose problems for cycling.

This study also shows that increasing complexity of the system provides several avenues for a chemical control over the electronic properties of OCC. Using chemical design principles, one can control the amount of the excited states in bi-OCC molecules and through symmetry and the degree of coupling between two metal centers. Since chemist's toolbox is essentially endless, many more handles and switches can be introduced into the system to control its electronic properties.

Acknowledgments – This work was funded by the NSF Center for Chemical Innovation Phase I (grant no. CHE-2221453), and NSF graduate fellowship DGE-2034835 to C.E.D. Computational resources were provided by ACCESS and UCLA IDRE.

REFERENCES

[1]L. D. Carr, D. DeMille, R. V. Krems, and J. Ye, "Cold and ultracold molecules: science, technology and applications," New Journal of Physics **11**, 055049 (2009).

[2]J. J. Hudson, D. M. Kara, I. Smallman, B. E. Sauer, M. R. Tarbutt, and E. A. Hinds, "Improved measurement of the shape of the electron," Nature **473**, 493–496 (2011).

[3]J. L. Bohn, A. M. Rey, and J. Ye, "Cold molecules: Progress in quantum engineering of chemistry and quantum matter," Science **357**, 1002–1010 (2017).

[4]D. J. Wineland, R. E. Drullinger, and F. L. Walls, "Radiation-pressure cooling of bound resonant absorbers," Physical Review Letters **40**, 1639 (1978).

[5]T. A. Isaev and R. Berger, "Polyatomic candidates for cooling of molecules with lasers from simple theoretical concepts," Phys. Rev. Lett. **116**, 063006 (2016).

[6]I. Kozyryev, L. Baum, K. Matsuda, and J. M. Doyle, "Proposal for laser cooling of complex polyatomic molecules," ChemPhysChem **17**, 3641–3648 (2016).

[7]I. Kozyryev, L. Baum, K. Matsuda, B. L. Augenbraun, L. Anderegg, A. P. Sedlack, and J. M. Doyle, "Sisyphus laser cooling of a polyatomic molecule," Phys. Rev. Lett. **118**, 173201 (2017).

[8]D. Mitra, N. B. Vilas, C. Hallas, L. Anderegg, B. L. Augenbraun, L. Baum, C. Miller, S. Raval, and J. M. Doyle, "Direct laser cooling of a symmetric top molecule," Science **369**, 1366–1369 (2020).

[9]M. L. Wall, K. Maeda, and L. D. Carr, "Simulating quantum magnets with symmetric top molecules," Annalen der Physik **525**, 845–865 (2013).

[10]V. V. Albert, J. P. Covey, and J. Preskill, "Robust encoding of a qubit in a molecule," Physical Review X **10**, 031050 (2020).

[11]I. Kozyryev, Z. Lasner, and J. M. Doyle, "Enhanced sensitivity to ultralight bosonic dark matter in the spectra of the linear radical sroh," Physical Review A **103**, 043313 (2021).

[12]M. V. Ivanov, F. H. Bangerter, and A. I. Krylov, "Towards a rational design of laser-coolable molecules: Insights from equation-of-motion coupled-cluster calculations," Phys. Chem. Chem. Phys. **21**, 19447–19457 (2019).

[13]M. V. Ivanov, S. Gulania, and A. I. Krylov, "Two cycling centers in one molecule: Communication by through-bond interactions and entanglement of the unpaired electrons," J. Phys. Chem. Lett. **11**, 1297–1304 (2020).

[14]M. Ivanov, A. I. Krylov, and S. Zilberg, "Long-range N-N bonding by Rydberg electrons," J. Phys. Chem. Lett. **11**, 2284–2290 (2020).

[15]M. V. Ivanov, F. H. Bangerter, P. Wójcik, and A. Krylov, "Towards ultracold organic chemistry: Prospects of laser cooling large organic molecules," J. Phys. Chem. Lett. **11**, 6670–6676 (2020).

[16]G. Z. Zhu, D. Mitra, B. L. Augenbraun, C. E. Dickerson, M. J. Frim, G. Lao, Z. D. Lasner, A. N. Alexandrova, W. C. Campbell, J. R. Caram, J. M. Doyle, and E. R. Hudson, "Functionalizing aromatic compounds with optical cycling centers," arXiv preprint arXiv:2202.01881 (2022).

[17]G. Zhu, D. Mitra, B. Augenbraun, C. Dickerson, M. Frim, G. Lao, Z. Lasner, A. Alexandrova, W. Campbell, J. Caram, J. Doyle, and E. Hudson, "Functionalizing aromatic compounds with optical cycling centres," Nat. Chem. **14**, 995–999 (2022).

[18]D. Mitra, Z. D. Lasner, G.-Z. Zhu, C. E. Dickerson, B. L. Augenbraun, A. D. Bailey, A. N. Alexandrova, W. C. Campbell, J. R. Caram, E. R. Hudson, and J. M. Doyle, "Pathway toward optical cycling and laser cooling of functionalized arenes," The Journal of Physical Chemistry Letters **13**, 7029–7035 (2022), pMID: 35900113.

[19]P. Yu, A. Lopez, W. A. Goddard, and N. R. Hutzler, "Multivalent optical cycling centers: towards control of polyatomics with multi-electron degrees of freedom," Physical Chemistry Chemical Physics **25**, 154–170 (2023).

[20]V. Zhelyazkova, A. Cournol, T. E. Wall, A. Matsushima, J. J. Hudson, E. Hinds, M. Tarbutt, and B. Sauer, "Laser cooling and slowing of caf molecules," Physical Review A **89**, 053416 (2014).

[21]C. Hallas, N. B. Vilas, L. Anderegg, P. Robichaud, A. Winnicki, C. Zhang, L. Cheng, and J. M. Doyle, "Optical trapping of a polyatomic molecule in an -type parity doublet state," Physical Review Letters **130**, 153202 (2023).

[22]M. J. O'Rourke and N. R. Hutzler, "Hypermetallic polar molecules for precision measurements," Physical Review A **100**, 022502 (2019).

[23]J. Kłos and S. Kotochigova, "Prospects for laser cooling of polyatomic molecules with increasing complexity," Physical Review Research **2**, 013384 (2020).

[24]L. Salem and C. Rowland, "The electronic properties of diradicals," Angew. Chem., Int. Ed. **11**, 92–111 (1972).

[25]V. Bonačić-Koutecký, J. Koutecký, and J. Michl, "Neutral and charged biradicals, zwitte-

rions, funnels in S_1, and proton translocation: Their role in photochemistry, photophysics, and vision," Angew. Chem., Int. Ed. **26**, 170–189 (1987).

[26]L. V. Slipchenko and A. I. Krylov, "Singlet-triplet gaps in diradicals by the spin-flip approach: A benchmark study," J. Chem. Phys. **117**, 4694–4708 (2002).

[27]A. I. Krylov, "The quantum chemistry of open-shell species," in *Reviews in Comp. Chem.*, Vol. 30, edited by A. L. Parrill and K. B. Lipkowitz (J. Wiley & Sons, 2017) pp. 151–224.

[28]N. Orms, D. R. Rehn, A. Dreuw, and A. I. Krylov, "Characterizing bonding patterns in diradicals and triradicals by density-based wave function analysis: A uniform approach," J. Chem. Theory Comput. **14**, 638–648 (2018).

[29]M. Head-Gordon, "Characterizing unpaired electrons from the one-particle density matrix," Chem. Phys. Lett. **372**, 508–511 (2003).

[30]C. E. Dickerson, H. Guo, A. J. Shin, B. L. Augenbraun, J. R. Caram, W. C. Campbell, and A. N. Alexandrova, "Franck-condon tuning of optical cycling centers by organic functionalization," Physical Review Letters **126** (2021), 10.1103/physrevlett.126.123002.

[31]M. Kasha, H. R. Rawls, and M. A. El-Bayoumi, "The exciton model in molecular spectroscopy," Pure & Appl. Chem. **11**, 371–392 (1965).

[32]A. S. Davydov, *Theory of Molecular Excitons* (McGraw-Hill, New York), 1962).

[33]S. Gulania, E. F. Kjønstad, J. F. Stanton, H. Koch, and A. I. Krylov, "Equation-of-motion coupled-cluster method with double electron-attaching operators: Theory, implementation, and benchmarks," J. Chem. Phys. **154**, 114115 (2021).

[34]A. I. Krylov, "Equation-of-motion coupled-cluster methods for open-shell and electronically excited species: The hitchhiker's guide to Fock space," Annu. Rev. Phys. Chem. **59**, 433–462 (2008).

[35]E. Epifanovsky, A. T. B. Gilbert, X. Feng, J. Lee, Y. Mao, N. Mardirossian, P. Pokhilko, A. F. White, M. P. Coons, A. L. Dempwolff, Z. Gan, D. Hait, P. R. Horn, L. D. Jacobson, I. Kaliman, J. Kussmann, A. W. Lange, K. U. Lao, D. S. Levine, J. Liu, S. C. McKenzie, A. F. Morrison, K. D. Nanda, F. Plasser, D. R. Rehn, M. L. Vidal, Z.-Q. You, Y. Zhu, B. Alam, B. J. Albrecht, A. Aldossary, E. Alguire, J. H. Andersen, V. Athavale, D. Barton, K. Begam, A. Behn, N. Bellonzi, Y. A. Bernard, E. J. Berquist, H. G. A. Burton, A. Carreras, K. Carter-Fenk, R. Chakraborty, A. D. Chien, K. D. Closser, V. Cofer-Shabica, S. Dasgupta, M. de Wergifosse, J. Deng, M. Diedenhofen, H. Do, S. Ehlert, P.-T. Fang, S. Fatehi, Q. Feng, T. Friedhoff, J. Gayvert, Q. Ge, G. Gidofalvi, M. Goldey, J. Gomes,

C. E. González-Espinoza, S. Gulania, A. O. Gunina, M. W. D. Hanson-Heine, P. H. P. Harbach, A. Hauser, M. F. Herbst, M. Hernández Vera, M. Hodecker, Z. C. Holden, S. Houck, X. Huang, K. Hui, B. C. Huynh, M. Ivanov, Á. Jász, H. Ji, H. Jiang, B. Kaduk, S. Kähler, K. Khistyaev, J. Kim, G. Kis, P. Klunzinger, Z. Koczor-Benda, J. H. Koh, D. Kosenkov, L. Koulias, T. Kowalczyk, C. M. Krauter, K. Kue, A. Kunitsa, T. Kus, I. Ladjánszki, A. Landau, K. V. Lawler, D. Lefrancois, S. Lehtola, R. R. Li, Y.-P. Li, J. Liang, M. Liebenthal, H.-H. Lin, Y.-S. Lin, F. Liu, K.-Y. Liu, M. Loipersberger, A. Luenser, A. Manjanath, P. Manohar, E. Mansoor, S. F. Manzer, S.-P. Mao, A. V. Marenich, T. Markovich, S. Mason, S. A. Maurer, P. F. McLaughlin, M. F. S. J. Menger, J.-M. Mewes, S. A. Mewes, P. Morgante, J. W. Mullinax, K. J. Oosterbaan, G. Paran, A. C. Paul, S. K. Paul, F. Pavošević, Z. Pei, S. Prager, E. I. Proynov, Á. Rák, E. Ramos-Cordoba, B. Rana, A. E. Rask, A. Rettig, R. M. Richard, F. Rob, E. Rossomme, T. Scheele, M. Scheurer, M. Schneider, N. Sergueev, S. M. Sharada, W. Skomorowski, D. W. Small, C. J. Stein, Y.-C. Su, E. J. Sundstrom, Z. Tao, J. Thirman, G. J. Tornai, T. Tsuchimochi, N. M. Tubman, S. P. Veccham, O. Vydrov, J. Wenzel, J. Witte, A. Yamada, K. Yao, S. Yeganeh, S. R. Yost, A. Zech, I. Y. Zhang, X. Zhang, Y. Zhang, D. Zuev, A. Aspuru-Guzik, A. T. Bell, N. A. Besley, K. B. Bravaya, B. R. Brooks, D. Casanova, J.-D. Chai, S. Coriani, C. J. Cramer, G. Cserey, A. E. DePrince, R. A. DiStasio, A. Dreuw, B. D. Dunietz, T. R. Furlani, W. A. Goddard, S. Hammes-Schiffer, T. Head-Gordon, W. J. Hehre, C.-P. Hsu, T.-C. Jagau, Y. Jung, A. Klamt, J. Kong, D. S. Lambrecht, W. Liang, N. J. Mayhall, C. W. McCurdy, J. B. Neaton, C. Ochsenfeld, J. A. Parkhill, R. Peverati, V. A. Rassolov, Y. Shao, L. V. Slipchenko, T. Stauch, R. P. Steele, J. E. Subotnik, A. J. W. Thom, A. Tkatchenko, D. G. Truhlar, T. Van Voorhis, T. A. Wesolowski, K. B. Whaley, H. L. Woodcock, P. M. Zimmerman, S. Faraji, P. M. W. Gill, M. Head-Gordon, J. M. Herbert, and A. I. Krylov, "Software for the frontiers of quantum chemistry: An overview of developments in the Q-Chem 5 package," J. Chem. Phys. **155**, 084801 (2021).

[36]A. I. Krylov, "Size-consistent wave functions for bond-breaking: The equation-of-motion spin-flip model," Chem. Phys. Lett. **338**, 375–384 (2001).

[37]D. Casanova and A. I. Krylov, "Spin-flip methods in quantum chemistry," Phys. Chem. Chem. Phys. **22**, 4326–4342 (2020).

[38]J. P. Perdew, M. Ernzerhof, and K. Burke, "Rationale for mixing exact exchange with density functional approximations," J. Chem. Phys. **105**, 9982–9985 (1996),

https://doi.org/10.1063/1.472933.

[39]S. Grimme, J. Anthony, S. Ehrlich, and H. Krieg, "A consistent and accurate ab initio parametrization of density functional dispersion correction (dft-d) for the 94 elements h-pu." J. Chem. Phys. **132**, 154104 (2010).

[40]D. Rappoport and F. Furche, "Property-optimized gaussian basis sets for molecular response calculations." J. Chem. Phys. **133**, 134105–1–134105–11 (2010).

[41]M. J. Frisch, G. W. Trucks, H. B. Schlegel, G. E. Scuseria, M. A. Robb, J. R. Cheeseman, G. Scalmani, V. Barone, G. A. Petersson, H. Nakatsuji, X. Li, M. Caricato, A. V. Marenich, J. Bloino, B. G. Janesko, R. Gomperts, B. Mennucci, H. P. Hratchian, J. V. Ortiz, A. F. Izmaylov, J. L. Sonnenberg, D. Williams-Young, F. Ding, F. Lipparini, F. Egidi, J. Goings, B. Peng, A. Petrone, T. Henderson, D. Ranasinghe, V. G. Zakrzewski, J. Gao, N. Rega, G. Zheng, W. Liang, M. Hada, M. Ehara, K. Toyota, R. Fukuda, J. Hasegawa, M. Ishida, T. Nakajima, Y. Honda, O. Kitao, H. Nakai, T. Vreven, K. Throssell, J. A. Montgomery, Jr., J. E. Peralta, F. Ogliaro, M. J. Bearpark, J. J. Heyd, E. N. Brothers, K. N. Kudin, V. N. Staroverov, T. A. Keith, R. Kobayashi, J. Normand, K. Raghavachari, A. P. Rendell, J. C. Burant, S. S. Iyengar, J. Tomasi, M. Cossi, J. M. Millam, M. Klene, C. Adamo, R. Cammi, J. W. Ochterski, R. L. Martin, K. Morokuma, O. Farkas, J. B. Foresman, and D. J. Fox, "Gaussian˜16 Revision C.01," (2016), gaussian Inc. Wallingford CT.

[42]Depending on molecular orientation, symmetry labels corresponding to the same orbital or vibrational mode may be different. Q-Chem's standard molecular orientation is different from that of Mulliken[50]. For example, Q-Chem would place water molecule in the xz plane instead of the yz. Consequently, for C_{2v} symmetry, b_1 and b_2 labels are flipped. More details can be found at http://iopenshell.usc.edu/resources/howto/symmetry/. To avoid confusion with different molecular orientations and relabeling the states, here we report the structures and symmetry labels following the Q-Chem's notations.

[43]H. Guo, C. Dickerson, A. J. Shin, C. Zhao, T. Atallah, J. R. Caram, W. Campbell, and A. Alexandrova, "Surface chemical trapping of optical cycling centers," Phys. Chem. Chem. Phys. , – (2020).

[44]C. E. Dickerson, A. N. Alexandrova, P. Narang, and J. P. Philbin, "Single molecule superradiance for optical cycling," arXiv preprint arXiv:2310.01534 (2023).

[45]P. Wójcik, T. Korona, and M. Tomza, "Interactions of benzene, naphthalene, and azulene with alkali-metal and alkaline-earth-metal atoms for ultracold studies," The Journal of

Chemical Physics **150**, 234106 (2019).

[46]D. Mitra and Z. L. et. al., "Pathway toward optical cycling and laser cooling of functionalized arenes," J. Phys. Chem. Lett. **13**, 7029–7035 (2022).

[47]T. Wang and A. I. Krylov, "The effect of substituents on singlet-triplet energy separations in meta-xylylene diradicals: Qualitative insights from quantitative studies," J. Chem. Phys. **123**, 104304–104310 (2005).

[48]T. Wang and A. I. Krylov, "Electronic structure of the two dehydro-meta-xylylene triradicals and their derivatives," Chem. Phys. Lett. **425**, 196–200 (2006).

[49]P. U. Manohar, L. Koziol, and A. I. Krylov, "Effect of a heteroatom on bonding patterns and triradical stabilization energies of 2,4,6-tridehydropyridine versus 1,3,5-tridehydrobenzene," J. Phys. Chem. A **113**, 2519–2599 (2009).

[50]R. S. Mulliken, "Report on notation for the spectra of polyatomic molecules," J. Chem. Phys. **23**, 1997–2011 (1955).